Am J Transl Res 2020;12(10):6509-6523
www.ajtr.org /ISSN:1943-8141/AJTR0117167

Original Article

Down-regulation of UL16-binding protein 3 mediated by interferon-gamma impairs immune killing in nasopharyngeal carcinoma

Lingling Guo[1,2*], Yu Chen[3,4,5*], Jing Wang[1,2*], Chuanben Chen[1,4,5]

[1]Department of Radiation Oncology of Head and Neck Cancers, Fujian Medical University Cancer Hospital & Fujian Cancer Hospital, Fuzhou 350000, China; [2]The School of Clinical Medicine, Fujian Medical University, Fuzhou 350000, China; [3]Department of Medical Oncology, Fujian Medical University Cancer Hospital & Fujian Cancer Hospital, Fuzhou 350000, China; [4]Cancer Bio-immunotherapy Center, Fujian Medical University Cancer Hospital & Fujian Cancer Hospital, Fuzhou 350000, China; [5]Fujian Key Laboratory of Translational Medicine, Fuzhou 350000, China. [*]Equal contributors.

Received June 29, 2020; Accepted September 13, 2020; Epub October 15, 2020; Published October 30, 2020

Abstract: Background: Nasopharyngeal carcinoma (NPC) is a malignant tumor characterized by a large number of tumor-infiltrating lymphocytes and high expression of programmed death ligand-1 (PD-L1). Interferon-gamma (IFN-γ) has proven to be the strongest inducers of PD-L1. This study aims at investigating the effect of IFN-γ on the expression of natural killer group 2, member D ligands (NKG2DLs), a series of immune-activating proteins, and their further effect on immune killing in NPC. Methods: RNA-seq data from the Gene Expression Omnibus database was downloaded and analyzed for the correlation between IFN-γ and NKG2DLs. IHC staining of clinical biopsy samples was performed to support the correlation between IFN-γ and ULBP3. Different NPC cell lines were treated with IFN-γ (100 U/ml) and the expression of PD-L1 and ULBP3 were detected at different time points. The 5-8F cell lines with PD-L1 over-expression and ULBP3 knockout were established and the T-cell cytotoxicity assay was performed to investigate the effect of ULPB3 on cytotoxicity. Results: Correlation analysis and IHC staining showed that the expression of ULBP3 had a significant negative correlation with IFN-γ in NPC patients. The vitro assays revealed that ULBP3 can be time-dependently down-regulated by IFN-γ. The cytotoxicity of $CD8^+$ T-cells that were co-cultured with ULBP3 knockout 5-8F cells was significantly impaired compared to wild type 5-8F cells. Conclusions: IFN-γ can significantly down-regulate the expression of ULBP3 in NPC. And the down-regulation of ULBP3 and the up-regulation of PD-L1 are both mediated by IFN-γ and may collectively play a role in the inhibition of immune killing in NPC.

Keywords: Immune killing, interferon-gamma (IFN-γ), nasopharyngeal carcinoma (NPC), programmed death ligand-1 (PD-L1), UL16-binding protein 3 (ULBP3)

Introduction

Nasopharyngeal carcinoma (NPC) is an Epstein-Barr Virus (EBV)-associated malignancy that is characterized by high level of tumor infiltrating lymphocytes (TILs) and high expression of programmed death ligand-1 (PD-L1) [1, 2]. At present, distant metastasis remains the main cause of treatment failure in NPC patients. As the efficacy of the first line platinum chemotherapy is limited, an effective systematic treatment after chemotherapy failure is particularly important. Based on the outcomes reported in the KEYNOTE-012 [3] and CheckMate 141 [4] studies, the Food and Drug Administration (FDA) accelerated the approval of pembrolizumab and nivolumab as a second-line treatment for recurrent and/or metastatic head and neck squamous cell carcinoma (r/m HNSCC) previously treated by chemotherapy. However, the efficacy of single PD-1 inhibitors is still limited in non-selective population of many advanced solid tumors [5-10], including the head and neck cancer [3, 4]. Although previous studies demonstrated that solid tumors that are infiltrated with a large number of $CD8^+$ T lymphocytes and express high levels of PD-L1 would have a better response to PD-1/PD-L1 inhibi-

tors [11], the objective response rate (ORR) of single PD-1 inhibitors in patients with PD-L1 positive r/m NPC is only 20% to 30% [12, 13].

The natural killer group 2, member D (NKG2D) receptor, is a type II transmembrane protein that is expressed on the surface of natural killer (NK) cells, $CD8^+$ T-cells, γδ T-cells, αβ T-cells, macrophages, and some $CD4^+$ T cells under certain selective stimuli or pathological conditions [14]. NKG2D ligands (NKG2DLs) are comprised of several MHC class I-like molecules including MHC class I-related genes A and B (MICA and MICB) and UL16-binding protein family (ULBP1-6) in humans. NKG2DLs are mainly expressed on tumor cells, macrophages, and dendritic cells (DCs) under different forms of cell stress, such as DNA damage, oxidative stress, heat-shock, and viral infection, including EBV infection [15-21]. Engagement of NKG2D and its ligands on target cells can increase the cytotoxicity of T-cells and the production of cytokines, playing an important role in both innate and adaptive immune responses [22].

Previous studies found that interferon gamma (IFN-γ), the strongest inducer of PD-L1, can regulate the expression of NKG2DLson the surface of melanoma, sarcoma, and other kinds of cancer cells [19, 23-27]. Based on these findings, we hypothesized that there is also an IFN-γ-mediated regulation of NKG2DLsin NPC that may affect the function of cytotoxic T-cells. To test our hypothesis, we analyzed the RNA-seq data from the GEO database and the assays of clinical biopsy samples and NPC cell lines. We verified that ULBP3, a member of NKG2DL family, can be significantly down-regulated by IFN-γ. Moreover, the knockout of ULPB3 with the overexpression of PD-L1 can significantly impair the cytotoxicity of antigen specific $CD8^+$ T-cells in nasopharyngeal carcinoma.

Methods

Analysis of the gene expression omnibus (GEO) database

RNA sequencing data of 113 patients with NPC were downloaded from the GEO database (https://www.ncbi.nlm.nih.gov/geo/query/acc.cgi?acc=GSE102349, accession number: GSE102349, accessed date: 20 December 2017). All gene expression quantification data were normalized to the RNA-seq value of the fragments per kilobase million (FPKM) (Supplementary Table 1). Expression of IFN-γ, PD-L1, and all NKG2D ligands were screened out and analyzed using the Spearman correlation in R Studio.

Clinical samples and follow-up

Fifty-seven cases of archived formalin-fixed and paraffin-embedded (FFPE) NPC biopsies were obtained from the Pathology Department, Fujian Cancer Hospital affiliated to Fujian Medical University. All tumor samples were isolated from consecutive untreated patients in 2008 who were pathologically diagnosed as non-keratinizing undifferentiated nasopharyngeal carcinoma stage III or IVA, and all received the standard treatment regimen of concurrent chemoradiotherapy in our center. Baseline characteristics including sex, age, T classification, N classification, and clinical stage were collected. The time to recurrence, metastasis, and death were recorded during the follow-ups. The follow-up cut-off time of all patients was October 1, 2018.

All sample and data collection and statistical analysis in this study were conducted in accordance with the Institutional Review Board of Fujian Medical University affiliated Cancer Hospital. Individual informed consent was waived based on the Ethical Board requirement for retrospective clinical studies. Patient records/information was anonymized and de-identified prior to analysis.

Immunohistochemistry

An anti-PD-L1 rabbit monoclonal antibody (SP142, Spring Bioscience), anti-CD8 rabbit monoclonal antibody (SP16, ZhongShanGoden-Bridge), and anti-ULBP3 rabbit polyclonal antibody (Abcam) were used to detect PD-L1, CD8, and ULBP3. Rabbit IgG (ab37415) was used as an isotype antibody control. Assessing and scoring were performed by two different certified pathologists. PD-L1 and ULBP3 were scored according to the combined positive score (CPS), which was defined as the total number of arbitrary intensity stained cells (including tumor cells, lymphocytes, and macrophages) divided by the total number of tumor cells [28]. For PD-L1, CPS<1 was considered negative, 1≤ CPS<20 was considered low, CPS≥20 was con-

sidered high. For ULBP3, CPS≤ or was considered negative, 1<CPS waswas considered low, CPS>5 was considered high. CD8 was scored according to the percentage of the area of interstitial lymphocytes stained with an arbitrary intensity to the total area of cells in the visual field [29]. Percentage ≤ Pe was considered negative, 20%< percentage ≤ erce was considered low, percentage >40% was considered high. The correlations between baseline characteristics, clinical outcomes and quantitative expression levels of CD8, PD-L1, and ULBP3 were analyzed using SPSS 21.0.

Cell culture

Three NPC cell lines (5-8F, CNE1, CNE2) were obtained from the Institute of Biochemistry and Cell Biology, Chinese Academy of Sciences, Shanghai. HEK293T was obtained from the Laboratory of Translational Medicine, Fujian Cancer Hospital. All cells were cultured in DMEM with 10% FBS and maintained in a humidified 5% CO_2 environment at 37°C. CNE1, CNE2, and 5-8F were treated with 100 U/ml exogenous IFN-γ (PeproTech, 300-02) and collected to determine the expression level of PD-L1 and ULBP3 after 0, 4, 12, and 24 h.

Flow cytometry

Cells were labeled with anti-human PD-L1 antibody (Biolegend, Catalog Number: 393605) and anti-human ULBP3 antibody (Santa Cruz Biotech, sc-390844), then subsequently labeled with FITC-conjugated goat anti-mouse IgG (Biolegend, 405305) and analyzed using NovoCyteflow cytometry (ACEA Biosciences, 1000) and FlowJo software. Cells were washed between the reactions in FACS buffer (1% FCS and 0.1% NaN_3 in PBS). Expression levels of PD-L1 and ULBP3 on the surface of tumor cells were represented as mean fluorescence intensity (MFI).

Western blotting

Cells were lysed in ice-cold RIPA buffer and 40 μg of protein was loaded for electrophoresis on 8%-12% denaturing SDS-PAGE gels. The blots were probed with the primary antibodies overnight at 4°C, followed by incubation with the appropriate secondary antibodies at room temperature for 1 h. The primary antibodies used were PD-L1 (1:1000, Cell Signaling Technology Inc, #13684), ULBP3 (1:1000, Santa Cruz Biotech Inc, sc-390844), GAPDH (1:1000, Abcam Inc, ab8245). The secondary antibodies used were HRP-conjugated goat anti-mouse IgG and goat anti-rabbit IgG.

Quantitative reverse-transcription polymerase chain reaction (qRT-PCR)

RNA isolated from cells was subjected to reverse transcription using Superscript III transcriptase (Invitrogen). qRT-PCR was conducted using a Bio-Rad CFX96 system with SYBR green to determine the mRNA expression level of genes of interest. Expression levels were normalized to 18s rRNA level. The following primers were used in qPCR, PD-L1, forward, 5'-AGTTCTGCGCAGCTTCCC-3'; PD-L1, reverse, 5'-GCGTTCAGCAAATGCCAG-3'; ULBP3, forward, 5'-CCTGATGCACAGGAAGAAGAG-3'; ULBP3, reverse, 5'-CTTAGCTCAACCCAAAGCCATA-3'; 18s, forward, 5'-CGACGACCCATTCGAACGTCT-3'; 18s, reverse, 5'-CTCTCCGGAATCGAA CCCTGA-3'.

Construction of cell lines with different phenotypes

The full-length PD-L1 gene sequence was obtained by PCR and made ligation-independent cloning (LIC) with pLV-EF1a-MCS-Flag-IRES-Bsd (Supplementary Figure 1A) processed by the BamHI/SmaI. PCR and sequencing were used to verify the obtained monoclone. Lentivirus particles were packaged by four-plasmid system (Supplementary Figure 1C-E) and transfected to human embryonic kidney (HEK) 293T cells. The overexpressed plasmid and the control plasmid were transfected into the 5-8F cells using the lipofectamine 2000 reagent. The transient expression of PD-L1 was detected by Western-blot or flow cytometry after 24 to 48 hours.

The ULBP3 sgRNA sequences were designed and selected out the first three with the highest scores for vector construction (**Table 1**). The vector Lenticrispr V2 (Supplementary Figure 1B) was cloned with three pairs of sgRNA after processed by BsmBI single cut linearization. The obtained monoclone was verified, packaged into lentivirus and transfected. The knockout plasmid and the control plasmid were transfected into 5-8F cells. The stably transfected cell lines were screened with 1 ug/ml Puromycin after 72 hours. Flow cytometry was

Table 1. The first 3 ULBP3 sgRNA sequences with the highest scores

Name of Prime	Sequence
ULBP3-sgRNA-F1	CACCGCTATTCGACTGGTCCGGGAC
ULBP3-sgRNA-R1	AAACGTCCCGGACCAGTCGAATAGC
ULBP3-sgRNA-F2	CACCGCAGGTACGGAAGAATCGCG
ULBP3-sgRNA-R2	AAACCGCGATTCTTCCGTACCTGC
ULBP3-sgRNA-F3	CACCGCTATTCGACTGGTCCGGGA
ULBP3-sgRNA-R3	AAACTCCCGGACCAGTCGAATAGC

used to detect the stable transgenic cells. Sequencing was used to evaluate the gene-editing of the genome.

Detection of specific CTL activity

The peripheral blood mononuclear cells (PBMCs) were isolated and induced to the mature dendritic cells (mDCs) by adding freeze-thaw 5-8F NPC cell antigen 100 ug/ml. The alloreactive $CD8^+$ T cells were induced by adding IFN-γ 20 μg/ml and IL-2 500 U/ml to the PBMCs. The 5-8F antigen-specific CTLs were attained by co-culturing $CD8^+$ T cells with mature DCs for 48 hours and sorted using $CD8^+$ T-cell isolation kit (MiltenyiBiotec) and VarioMACS Separator (MiltenyiBiotec). Flow cytometry was used to isolate and detect the purity of the $CD8^+$ T-cells. The 5-8F cell lines with different membrane phenotypes were stained with Carboxyfluorescein succinimidyl ester (CFSE) and co-cultured with 5-8F antigen-specific $CD8^+$ T-cells at different ratios of effector cells to target cells (1:1, 5:1 and 10:1). The spontaneous apoptosis of 5-8F cell lines was used the tumor cell spontaneous control. The suspended cells and adherent cells were collected and evaluated by flow cytometry after 8 hours.

Statistics

All group data are represented as the mean ± SD. The differences in mean values between the two groups were compared using a two-tailed unpaired Student's t-test. Between multiple groups, the data were analyzed using an analysis of variance (ANOVA) with the Bonferroni correction. A *P* value less than or equal to 0.05 was considered as statistically significant. R studio, Prism (GraphPad Software Inc.) and SPSS21.0 (International Business Machines Corporation) were used for the statistical analyses.

Results

Correlations among NKG2DL, PD-L1 and IFN-γ at mRNA level in NPC

In 113 patients with NPC obtained from GEO database, correlation analysis (**Figure 1**) showed that IFN-γ was significantly positively correlated with PD-L1 (R=0.35, P<0.001) and MICB (R=0.412, P<0.001). Given the reported that NKG2DLs are associated with the clearance of virus [22], we speculated that the positive correlation between IFN-γ and MICB could due to the infiltration of a large number of TILs in the inflammatory phase, which were involved in the clearance of Epstein-Barr virus. Meanwhile, IFN-γ was significantly negatively correlated with UBLP1 (R=-0.241, P=0.01), UBLP3 (R=-0.3, P=0.001), ULBP5 (R=-0.19, P=0.04), and ULBP6 (R=-0.31, P<0.001). Given that ULBP6 is mainly related to virus infection and autoimmune diseases [30], we focused on ULBP3 in the following assays.

Correlations among ULBP3, PD-L1 and $CD8^+$ T-cells at protein level in NPC patients

In this study, 57 patients with NPC were enrolled. Their baseline characteristics, clinical outcomes and survival analysis are shown in the supplemental materials (Supplementary Tables 2, 3, 5, Supplementary Figure 5). IHC showed that PD-L1 was mainly distributed on the membrane of tumor cells (TCs) presenting circular or linear staining, and a few were scattered in the cytoplasm of interstitial immune cells (ICs). The intensity of staining was yellow to brown. CD8 was distributed in the cytoplasm of infiltrating ICs in the stroma, stained dark yellow to dark brown. ULBP3 was found mostly in the cytoplasm of ICs and a very small amount was found in TCs, showing yellow to brown appearance.

According to the predefined criteria, the positive rates of expression of PD-L1, CD8 and ULBP3 protein among 57 cases of NPC samples were 57.9%, 93.0%, and 38.6% respectively (Supplementary Table 4). The rate of high expression was 31.6%, 50.9%, and 29.8% respectively. Spearman rank correlation analysis (**Tables 2A-C**) showed that the expression level of PD-L1 protein was positively correlated with CD8 protein (R<0.36, P<0.05) and negatively correlated with ULBP3 protein (R=0.44,

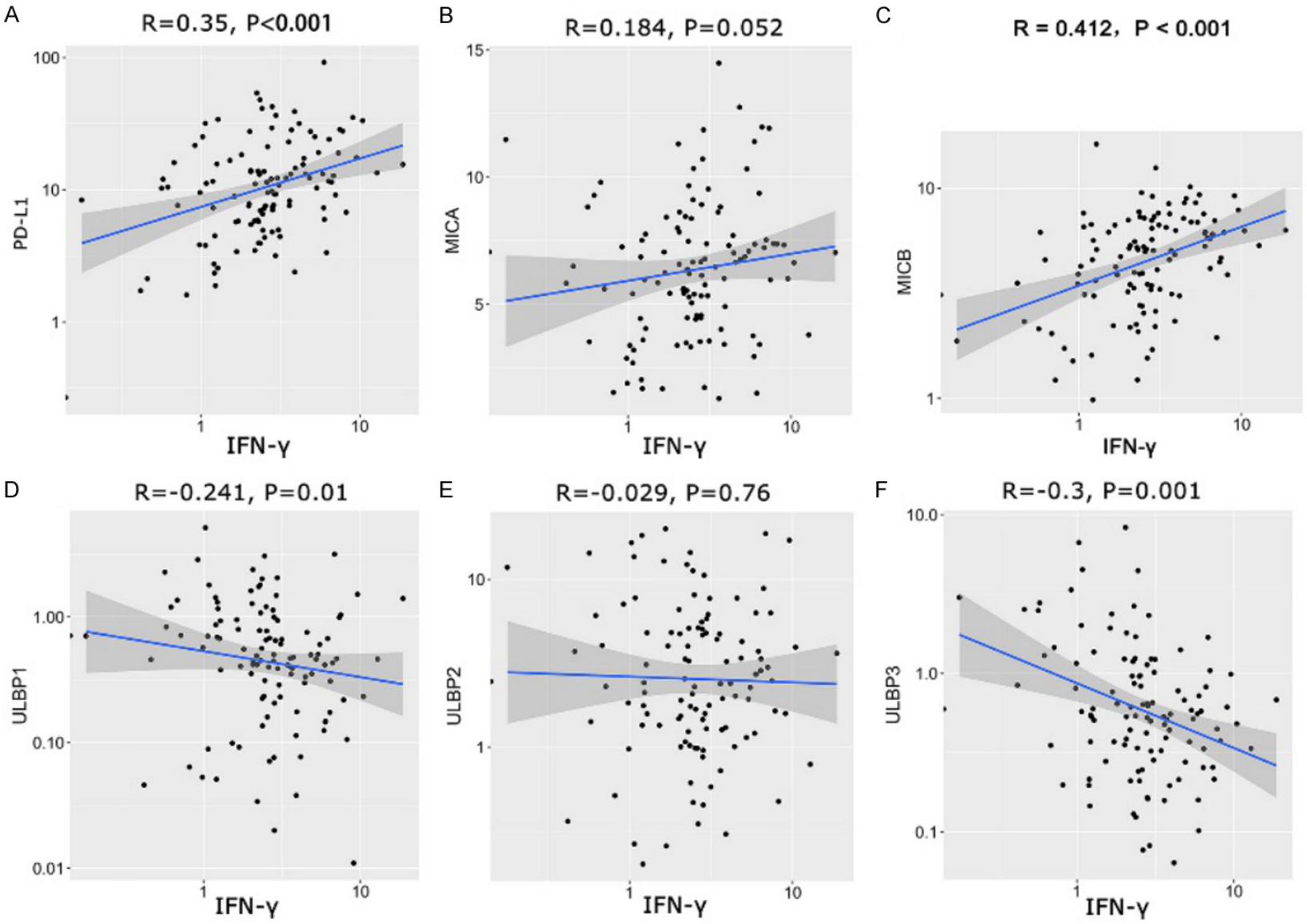
A
R=0.35, P<0.001
PD-L1
IFN-γ
B
R=0.184, P=0.052
MICA
IFN-γ
C
R = 0.412, P < 0.001
MICB
IFN-γ
D
R=-0.241, P=0.01
ULBP1
IFN-γ
E
R=-0.029, P=0.76
ULBP2
IFN-γ
F
R=-0.3, P=0.001
ULBP3
IFN-γ

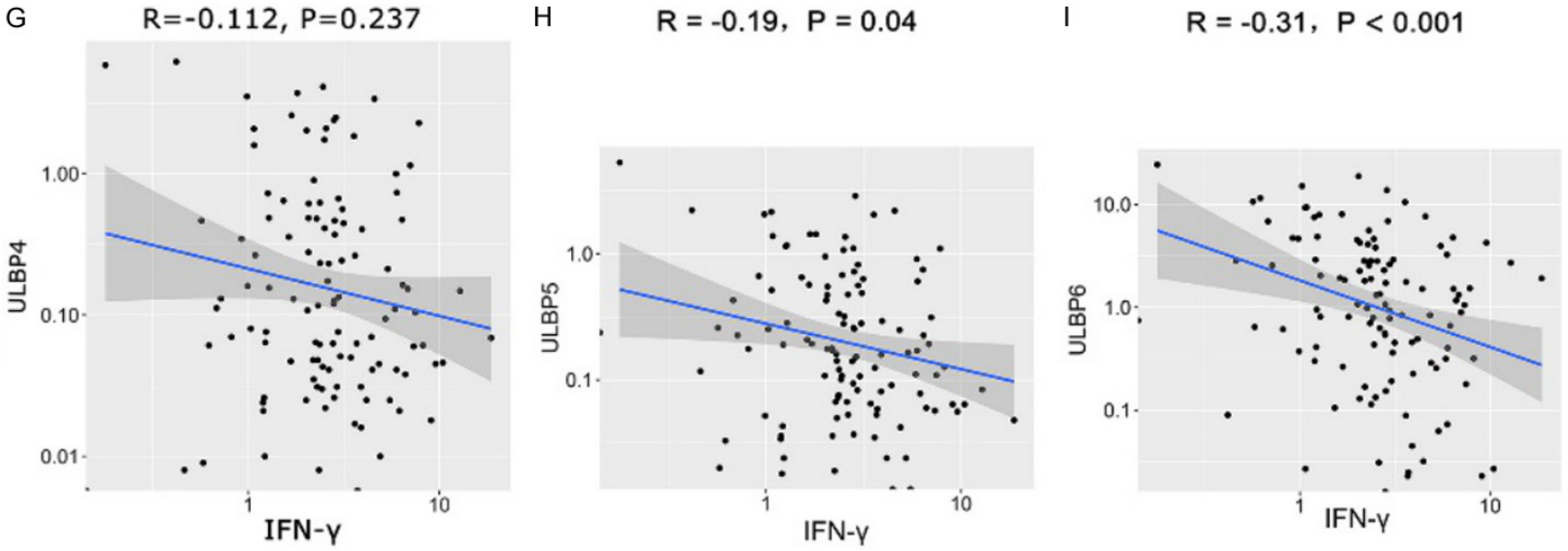

Figure 1. IFN-γ was positively related to PD-L1, MICB and negatively related to some ULBPs. The RNA-seq data of 113 patients with NPC downloaded from the GEO database (GSE102349) were analyzed by Spearman correlation analysis. At the mRNA level, IFN-γ had significantly positive correlations with (A) PD-L1 and (C) MICB. IFN-γ had significant negative correlations with (D) ULBP1, (F) ULBP3, (H) ULBP5 and (I) ULBP6, and no significant correlations with (B) MICA, (E) ULBP2 and (G) ULBP4. The correlation between IFN-γ and MICB indicated that MICB might play a role in the infection and clearance of EBV.

Table 2A. Spearman rank correlation analysis between PD-L1 and CD8

		CD8 expression			Total	χ^2	*P*-value	Spearman R-value	*P*-value
		negative	Low	High					
PD-L1 expression	negative	10	4	11	25	12.681	0.013	0.356	0.007
	Low	5	5	4	14				
	High	0	4	14	18				
	Total	15	13	29	57				

Table 2B. Spearman rank correlation analysis between PD-L1 and ULBP3

		ULBP3 expression		Total	χ^2	*P*-value	Spearman R-value	*P*-value
		Negative/low	High					
PD-L1 expression	Negative/low	22	17	39	11.181	0.000	-0.443	0.001
	High	18	0	18				
	Total	40	17	57				

Table 2C. Spearman rank correlation analysis between CD8 and ULBP3

		ULBP3 expression			Total	χ^2	*P*-value	Spearman R-value	*P*-value
		negative	Low	High					
CD8 expression	negative	9	1	5	15	1.122	0.891	-0.013	0.921
	Low	8	2	3	13				
	High	18	2	9	29				
	Total	35	5	17	57				

P<0.001). At the same time, we found that there is a medium level of exclusiveness in the special distribution of PD-L1 and ULBP3 (**Figure 2**).

Correlations among ULBP3, PD-L1, and IFN-γ in NPC cell lines

Three NPC cell lines, 5-8F, CNE1, and CNE2, which were preserved in our laboratory, were selected to study the regulatory effect of IFN-γ on the expression of PD-L1 and ULBP3 in NPC. After being exposed to IFN-γ at a dose of 100 ng/ml all three cell lines showed a significantly higher expression of PD-L1 (P<0.05) and a significantly lower expression of ULBP3 (P<0.05). With exposure to IFN-γ, the expression of PD-L1 was significantly up-regulated and the expression of ULBP3 was significantly down-regulated at both RNA and protein levels in all cell lines (**Figure 3**).

Detection of cytolytic activity of CD8$^+$ T cells against 5-8F cell lines with different phenotypes

Three 5-8F cell lines with different phenotypes were constructed in vitro: 1) the PD-L1^{oe}-5-8F cell line that was transiently transfected with a PD-L1 expression vector (Supplementary Figure 2A-C); 2) the ULBP3^{ko}-5-8F cell line that was stably transfected with the ULBP3 knockout vector (Supplementary Figures 2D, 2E, 3); 3) the ULBP3^{ko}PD-L1^{oe}-5-8F cell line that had both a knockout of ULBP3 and overexpression of PD-L1. The wild-type 5-8F cell line was used as a control.

The 5-8F-specific CTLs were obtained by co-culturing CD8$^+$ T-cells with mature DC which had been co-cultured with 5-8F cells, then sorted and purified by a flow cytometry VarioMACS system. The results of FC showed that the proportion of 5-8F-specific CD8$^+$ T-cells increased from 49.13% to 92.57% (Supplementary Figure 4A and 4B).

We co-cultured the various 5-8F cell lines with 5-8F-specific CD8$^+$ T-cells and identified the cytolysis of tumor cells using CFSE-PI-flow cytometry. The results show that at a 1:1 ratio of effector cells to target cells, the cytolysis of tumor cells in the PD-L1^{oe}-5-8F, ULBP3^{ko}-5-8F, ULBP3^{ko}-PD-L1^{oe}-5-8F, and control groups were, respectively, 18.49%, 20.13%, 12.56%,

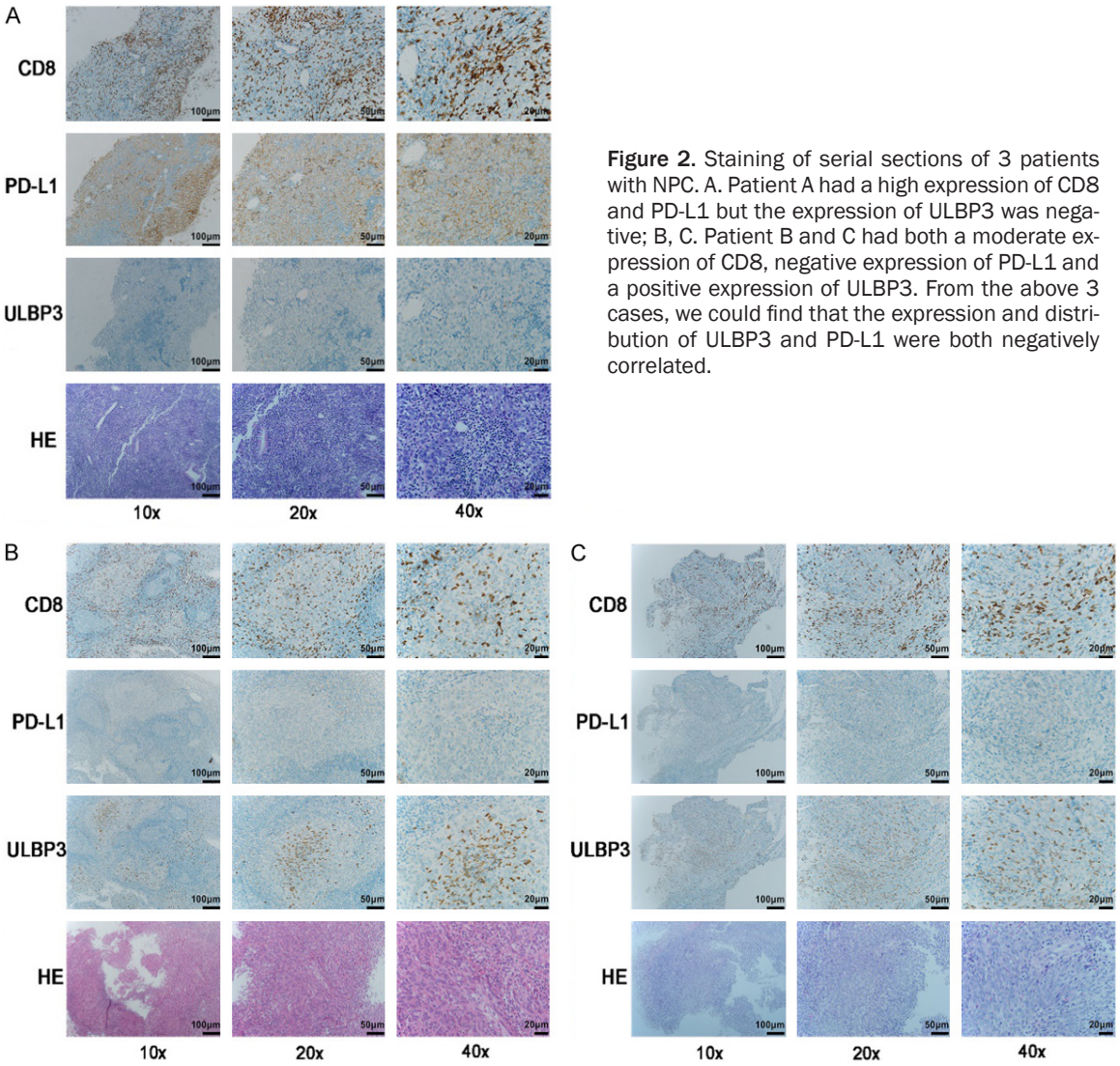

Figure 2. Staining of serial sections of 3 patients with NPC. A. Patient A had a high expression of CD8 and PD-L1 but the expression of ULBP3 was negative; B, C. Patient B and C had both a moderate expression of CD8, negative expression of PD-L1 and a positive expression of ULBP3. From the above 3 cases, we could find that the expression and distribution of ULBP3 and PD-L1 were both negatively correlated.

and 23.41% (**Figure 4A-D**); at a 5:1 ratio of effector cells to target cells, the cytolysis rates were 34.28%, 33.63%, 27.92%, and 46.88% respectively (**Figure 4E-H**); and at a 10:1 ratio of effector cells to target cells, the cytolysis rates were 46.67%, 42.62%, 38.65%, and 69.02% respectively (**Figure 4I-L**).

Results of t-tests suggested that both the knockout of the ULBP3 gene and overexpression of the PD-L1 gene could decrease the cytolytic ability of $CD8^+$ T-cells to 5-8F cells. Moreover, the combination of ULBP3-knockout and overexpression PD-L1 significantly decreased the cytolytic ability of $CD8^+$ T-cells (**Figure 4N-P**). In addition, with the increase of the ratio of effector cells to target cells, the cytolytic efficiency of $CD8^+$ T-cells against 5-8F cells was significantly increased (**Figure 4M**).

Discussion

In our study, we found in vitro that IFN-γ can significantly up-regulate PD-L1 and down-regulate ULBP3 in the microenvironment of NPC. Moreover, the overexpression of PD-L1 and the knockout of ULBP3 will both impair the cytotoxicity of antigen-specific $CD8^+$ T-cells, and the PD-L1 overexpression combining with ULBP3 knockout will most significantly PD-L1 weaken the killing activity of CTLs.

Many previous studies demonstrated that IFN-γ released by activated $CD8^+$ T-cells, NK cells, and NKT cells is the strongest inducing factor of PD-L1 [31-33]. In our study, we also confirmed that there is an IFN-γ-dependent up-regulation of PD-L1 in NPC. Moreover, some researchers indicated that the binding of IFN-γ

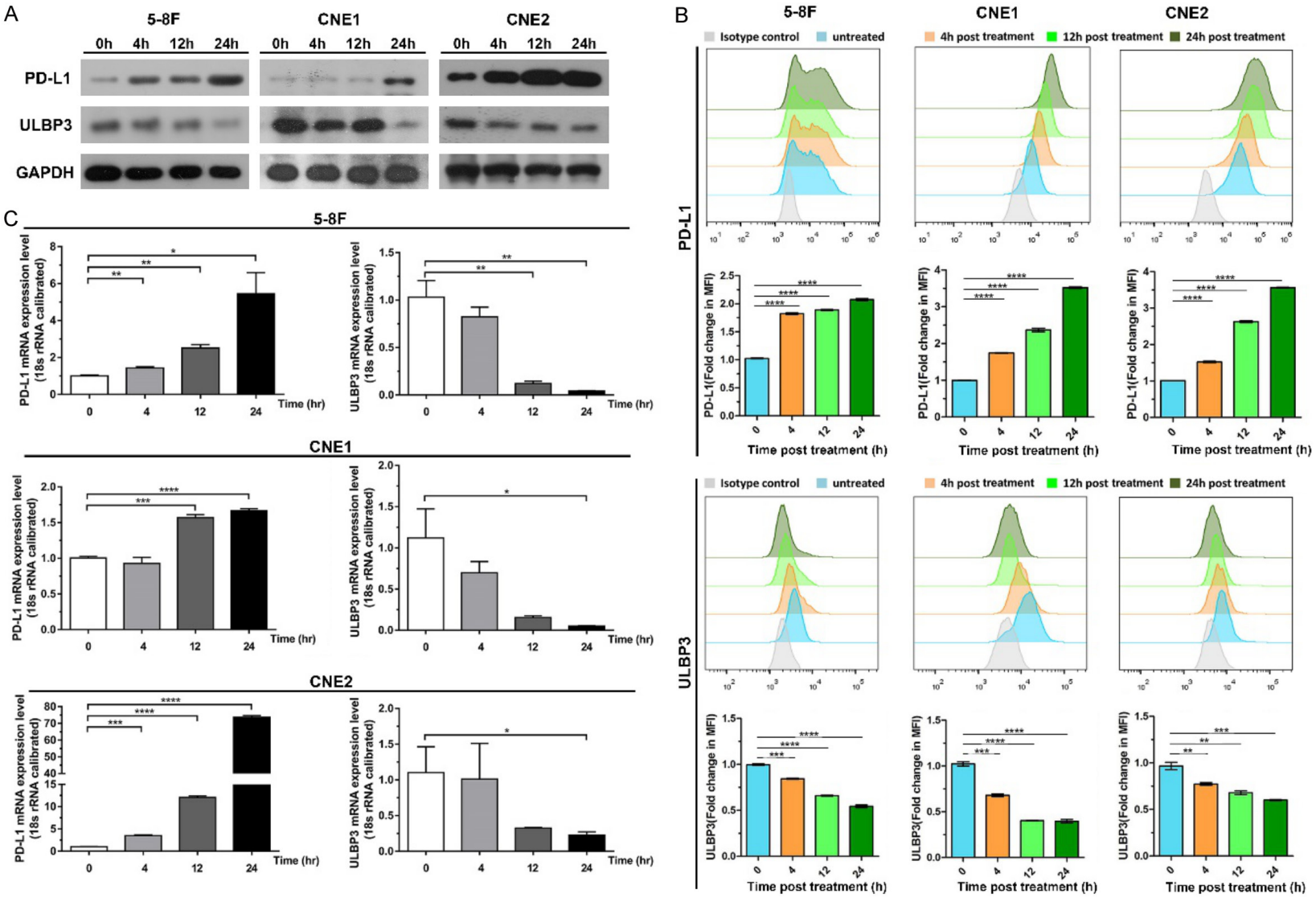

Figure 3. IFN-γ up-regulated PD-L1 and down-regulated ULBP3 in NPC cell lines. The 5-8F, CNE1, and CNE2 cell lines were treated by exogenous recombinant IFN-γ and detected the expression of PD-L1 and ULBP3 respectively when 0, 4, 12 and 24 h after treatment. From (A-C), results of Western blotting, FACS, and real-time PCR showed that IFN-γ can significantly up-regulate the expression of PD-L1 and down-regulate the expression of ULBP3. Moreover, the effect of IFN-γ was time-dependent. *P<0.05, **P<0.01, ***P<0.001, ****P<0.0001.

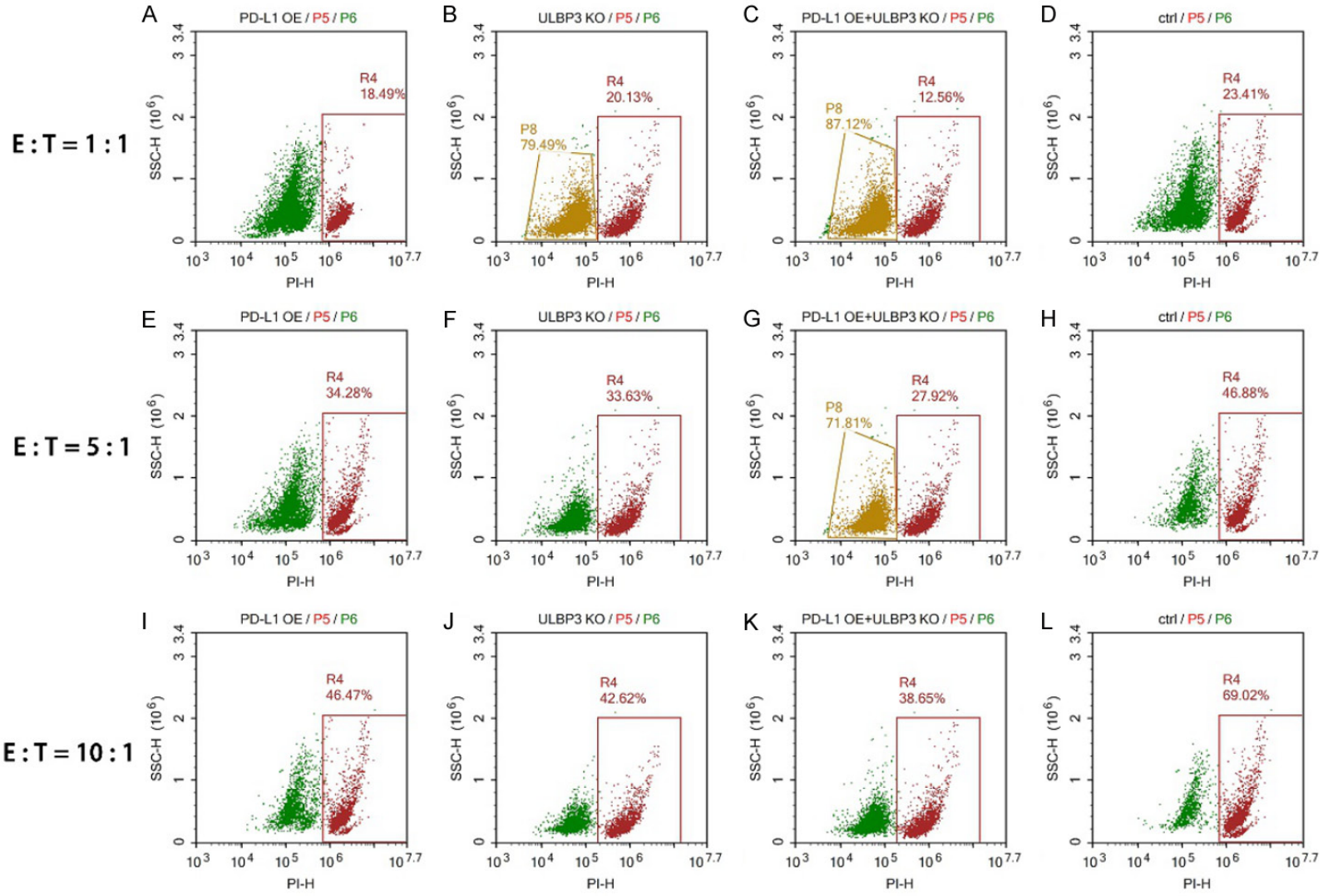
A
PD-L1 OE / P5 / P6
R4
18.49%
B
ULBP3 KO / P5 / P6
R4
20.13%
P8
79.49%
C
PD-L1 OE+ULBP3 KO / P5 / P6
R4
12.56%
P8
87.12%
D
ctrl / P5 / P6
R4
23.41%
E:T=1:1
E
PD-L1 OE / P5 / P6
R4
34.28%
F
ULBP3 KO / P5 / P6
R4
33.63%
G
PD-L1 OE+ULBP3 KO / P5 / P6
R4
27.92%
P8
71.81%
H
ctrl / P5 / P6
R4
46.88%
E:T=5:1
I
PD-L1 OE / P5 / P6
R4
46.47%
J
ULBP3 KO / P5 / P6
R4
42.62%
K
PD-L1 OE+ULBP3 KO / P5 / P6
R4
38.65%
L
ctrl / P5 / P6
R4
69.02%
E:T=10:1
SSC-H (10^6)
PI-H

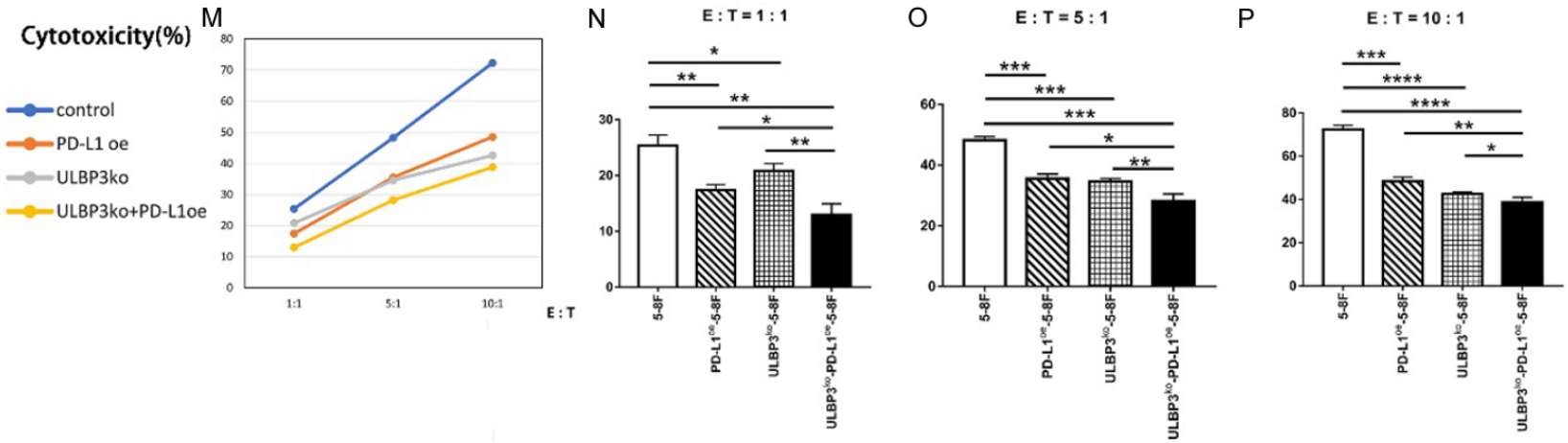

Figure 4. PD-L1 overexpression and ULBP3 knockout impaired the cytotoxic of 5-8F specific $CD8^+$ T-cells. Three kinds of 5-8F cell lines ($PD\text{-}L1^{oe}$, $ULBP3^{ko}$, $PD\text{-}L1^{oe}$+$ULBP3^{ko}$) with different phenotypes and the control cell line were co-cultured with 5-8F antigen-specific $CD8^+$ T-cells at different ratios of effector cells to target cells (1:1, 5:1 and 10:1). The cytotoxicity of $CD8^+$ T-cells was assessed by FACS. A-D. Death rates of tumor cells at 1:1 ratio of E:T in $PD\text{-}L1^{oe}$-5-8F, $ULBP3^{ko}$-5-8F, $ULBP3^{ko}$-$PD\text{-}L1^{oe}$-5-8F cell lines, and blank control group; E-H. Death rates of tumor cells at 5:1 ratio of E:T in different cell lines; I-L. Death rates of tumor cells at 10:1 ratio of E:T in different cell lines; M. Cytotoxicity of CTLs on tumor cells was up-regulated as the ratio of E:T raised; N-P. Comparation of cytotoxicity of CTLs on each cell line at different ratios of E:T. *P<0.05, **P<0.01, ***P<0.001, ****P<0.0001.

to its receptor can activate the classical JAKs-STATs pathway and induce the up-regulation of interferon regulatory factor 1 (IRF-1), which finally enters the cell nucleus and promotes the transcription and expression of PD-L1 [34].

Similar to PD-L1, ULBP3 is also proven to be a type of stress-induced protein that is widely expressed on tumor cells, activated T-cells, macrophages, and during virus infection, malignant transformation, or oxidative stress [35, 36]. Some researchers found that tumor cells can down-regulate the expression of NKG2DL on their surface through a variety of pathways, and the IFN-γ was one of the important regulatory factors. Zhang et al. confirmed that IFN-γ can up-regulate the synthesis of matrix metalloproteinases (MMPs), which promotes the shearing and shedding of membrane MICA protein and increases the level of soluble MICA protein [27]. Yadav et al. found that IFN-γ could down-regulate the expression of MICA at a post-transcriptional level by increasing the miR-520b in many tumors [26]. In addition, Schwinn et al. demonstrated that IFN-γ can directly down-regulate the transcription of NKG2DL and STAT1 protein that play an important role in this process [25]. Consistent with previous findings, we also found that the expression of many NKG2DLs were down-regulated by IFN-γ in NPC, the most significant of which was ULBP3.

All of these results indicated that there is an IFN-γ induced up-regulation of PD-L1 and a down-regulation of ULBP3 in NPC. The mechanisms include a down-regulation at both the transcription and protein levels, and the promotion of the secretion of membrane proteins. Combined with the previous results, we speculate that these two molecular events are likely to occur through a common signal pathway, the JAKs-STATs pathway. More in vivo experiments are needed to explore and confirm this molecular mechanism. We also found that there is an exclusiveness in special distribution between ULBP3 and PD-L1, which indicated that there may exist an inhibitive interaction between UBLP3 and PD-L1 proteins. Those conjectures still need to be verified by further experiments.

The $CD8^+$ T-cell response plays an important role in inhibiting tumor development, but their cytolytic function against tumor cells is regulated by many factors, including the expression and interaction of the NKG2D receptor and its ligands [37]. Previous studies have confirmed that the down-regulation of NKG2DLs can decrease the cytolytic activity of NKG2D-positive effector immune cells, suppress both the innate and adaptive immune responses, and finally promote immune escape [38-40]. Zhang et al. blocked the NKG2D receptors on immune cells with monoclonal antibodies and found that their cytolytic function against tumor cells was reduced, which shows that IFN-γ can decrease the expression of NKG2DLs and impair the function of immune cells mediated by NKG2DL [41]. In our study, we constructed three kinds of 5-8F cell lines with different phenotypes of ULBP3 and PD-L1 and found that the overexpression of PD-L1 and the knockout of ULBP3 on 5-8F cells could impair the killing function of specific $CD8^+$ T-cells. Moreover, those tumor cells which also had PD-L1 overexpression and ULBP3 knockout showed the strongest resistance to $CD8^+$ T-cells. We also found lack of ULBP3 and high expression of PD-L1 in a NPC patient with primary resistance to PD-1 inhibitors (Supplementary Figure 6). These results suggest that the lack of ULBP3 might have a synergistic effect with high expression of PD-L1 on the immune resistance of nasopharyngeal carcinoma cells.

Conversely, some researchers found that increasing the expression of NKG2DLs on tumor cells can enhance the cytotoxic effect of NK cells both in vivo and in vitro [42-44]. Andreas et al. [45] and Xu et al. [46] found that the up-regulation of expression of NKG2DLs could enhance the cytotoxic ability of immune cells. Xu et al. also proved that the expression of ULBP4 could improve the cytotoxic function of immune cells, using the killing activity experiments and NPC cell lines with different expression levels of ULBP4 [46]. However, some researchers found that when massive expression and shedding of NKG2DL occur, the promotion of immune function mediated by NKG2D will be counterweighed and the population of immunosuppressive T-cells will be expanded [47]. This suggests that the shedding of ULBP3 maybe one other mechanism responsible for impairing the killing activity of $CD8^+$ T-cells.

In summary, clinical data has shown that a single PD-1 inhibitor has only a limited effect on patients with recurrent and/or metastatic NPC, even those patients with a high expression of PD-L1 [12, 13]. Our study provides a new view

that the IFN-γ mediated lack or suppressed expression of ULBP3 and high expression of PD-L1 could be the important markers which could promote the immune escape and promote immune resistance in the NPC microenvironment. The patients with PD-L1 positive and ULBP3-low expression could be a unique subgroup of immune escapees.

Acknowledgements

This work was supported by research projects for Startup Fund for scientific research, Fujian Medical University [grant number 2017XQ12-10], Science and Technology Program of Fujian Province, China [grant number 2018Y2003], Natural Science Foundation of Fujian Province [grant numbers 2017J01259, 2018J01267, 2019J01052066], Fujian Provincial Health and Family Planning Research Talent Training Program [grant numbers 2018-ZQN-13, 2018-CX-11], Joint Funds for the Innovation of Science and Technology, Fujian province [grant number 2017Y9077], and the National Clinical Key Specialty Construction Program. Additionally, we thank Mr. Huaibo Sun (Genecast Biotechnology Co. Ltd., Beijing, China) for his help in analyzing RNA-seq data from GEO database. We thank Dr. Zhen Wang (Anti-hela Biological Technology Trade Co. Ltd., Xiamen, China) for his technical help in vitro assays. We also appreciate Dr. Jianping Lu and Dr. Weifeng Zhu (both from Pathology Department, Fujian Medical University Affiliated Cancer Hospital, Fuzhou, China) for their professional advice in immunohistochemistry staining and assessment.

Disclosure of conflict of interest

None.

Address correspondence to: Chuanben Chen, Department of Radiation Oncology of Head and Neck Cancers, Fujian Cancer Hospital & Fujian Medical University Cancer Hospital, No. 420, Fuma Road, Jinan District, Fuzhou 350014, China. E-mail: ccbben@126.com

References

[1] Chua MLK, Wee JTS, Hui EP and Chan ATC. Nasopharyngeal carcinoma. Lancet 2016; 387: 1012-1024.

[2] Larbcharoensub N, Mahaprom K, Jiarpinitnun C, Trachu N, Tubthong N, Pattaranutaporn P, Sirachainan E and Ngamphaiboon N. Characterization of PD-L1 and PD-1 expression and CD8+ tumor-infiltrating lymphocyte in epstein-barr virus-associated nasopharyngeal carcinoma. Am J Clin Oncol 2018; 41: 1204-1210.

[3] Seiwert TY, Burtness B, Mehra R, Weiss J, Berger R, Eder JP, Heath K, McClanahan T, Lunceford J, Gause C, Cheng JD and Chow LQ. Safety and clinical activity of pembrolizumab for treatment of recurrent or metastatic squamous cell carcinoma of the head and neck (KEYNOTE-012): an open-label, multicentre, phase 1b trial. Lancet Oncol 2016; 17: 956-965.

[4] Ferris RL, Blumenschein G Jr, Fayette J, Guigay J, Colevas AD, Licitra L, Harrington K, Kasper S, Vokes EE, Even C, Worden F, Saba NF, Iglesias Docampo LC, Haddad R, Rordorf T, Kiyota N, Tahara M, Monga M, Lynch M, Geese WJ, Kopit J, Shaw JW and Gillison ML. Nivolumab for recurrent squamous-cell carcinoma of the head and neck. N Engl J Med 2016; 375: 1856-1867.

[5] Garon EB, Rizvi NA, Hui R, Leighl N, Balmanoukian AS, Eder JP, Patnaik A, Aggarwal C, Gubens M, Horn L, Carcereny E, Ahn MJ, Felip E, Lee JS, Hellmann MD, Hamid O, Goldman JW, Soria JC, Dolled-Filhart M, Rutledge RZ, Zhang J, Lunceford JK, Rangwala R, Lubiniecki GM, Roach C, Emancipator K and Gandhi L. Pembrolizumab for the treatment of non-small-cell lung cancer. N Engl J Med 2015; 372: 2018-2028.

[6] Borghaei H, Paz-Ares L, Horn L, Spigel DR, Steins M, Ready NE, Chow LQ, Vokes EE, Felip E, Holgado E, Barlesi F, Kohlhaufl M, Arrieta O, Burgio MA, Fayette J, Lena H, Poddubskaya E, Gerber DE, Gettinger SN, Rudin CM, Rizvi N, Crino L, Blumenschein GR Jr, Antonia SJ, Dorange C, Harbison CT, Graf Finckenstein F and Brahmer JR. Nivolumab versus docetaxel in advanced nonsquamous non-small-cell lung cancer. N Engl J Med 2015; 373: 1627-1639.

[7] Brahmer J, Reckamp KL, Baas P, Crino L, Eberhardt WE, Poddubskaya E, Antonia S, Pluzanski A, Vokes EE, Holgado E, Waterhouse D, Ready N, Gainor J, Aren Frontera O, Havel L, Steins M, Garassino MC, Aerts JG, Domine M, Paz-Ares L, Reck M, Baudelet C, Harbison CT, Lestini B and Spigel DR. Nivolumab versus docetaxel in advanced squamous-cell non-small-cell lung cancer. N Engl J Med 2015; 373: 123-135.

[8] Motzer RJ, Escudier B, McDermott DF, George S, Hammers HJ, Srinivas S, Tykodi SS, Sosman JA, Procopio G, Plimack ER, Castellano D, Choueiri TK, Gurney H, Donskov F, Bono P, Wagstaff J, Gauler TC, Ueda T, Tomita Y, Schutz FA, Kollmannsberger C, Larkin J, Ravaud A,

Simon JS, Xu LA, Waxman IM and Sharma P. Nivolumab versus everolimus in advanced renal-cell carcinoma. N Engl J Med 2015; 373: 1803-1813.

[9] Larkin J, Chiarion-Sileni V, Gonzalez R, Grob JJ, Cowey CL, Lao CD, Schadendorf D, Dummer R, Smylie M, Rutkowski P, Ferrucci PF, Hill A, Wagstaff J, Carlino MS, Haanen JB, Maio M, Marquez-Rodas I, McArthur GA, Ascierto PA, Long GV, Callahan MK, Postow MA, Grossmann K, Sznol M, Dreno B, Bastholt L, Yang A, Rollin LM, Horak C, Hodi FS and Wolchok JD. Combined nivolumab and ipilimumab or monotherapy in untreated melanoma. N Engl J Med 2015; 373: 23-34.

[10] Robert C, Schachter J, Long GV, Arance A, Grob JJ, Mortier L, Daud A, Carlino MS, McNeil C, Lotem M, Larkin J, Lorigan P, Neyns B, Blank CU, Hamid O, Mateus C, Shapira-Frommer R, Kosh M, Zhou H, Ibrahim N, Ebbinghaus S and Ribas A. Pembrolizumab versus ipilimumab in advanced melanoma. N Engl J Med 2015; 372: 2521-2532.

[11] Teng F, Meng X, Kong L and Yu J. Progress and challenges of predictive biomarkers of anti PD-1/PD-L1 immunotherapy: a systematic review. Cancer Lett 2018; 414: 166-173.

[12] Hsu C, Lee SH, Ejadi S, Even C, Cohen RB, Le Tourneau C, Mehnert JM, Algazi A, van Brummelen EMJ, Saraf S, Thanigaimani P, Cheng JD and Hansen AR. Safety and antitumor activity of pembrolizumab in patients with programmed death-ligand 1-positive nasopharyngeal carcinoma: results of the KEYNOTE-028 study. J Clin Oncol 2017; 35: 4050-4056.

[13] Delord JP, Hollebecque A, Boer JPD, Greve JD, Machiels JPH, Leidner RS, Ferris RL, Rao S, Soumaoro I, Cao ZA, Kang H and Topalian SL. An open-label, multicohort, phase I/II study to evaluate nivolumab in patients with virus-associated tumors (CheckMate 358): efficacy and safety in recurrent or metastatic (R/M) nasopharyngeal carcinoma (NPC). J Clin Oncol 2017; 35: 6025-6025.

[14] Raulet DH, Gasser S, Gowen BG, Deng W and Jung H. Regulation of ligands for the NKG2D activating receptor. Annu Rev Immunol 2013; 31: 413-441.

[15] Stojanovic A, Correia MP and Cerwenka A. The NKG2D/NKG2DL axis in the crosstalk between lymphoid and myeloid cells in health and disease. Front Immunol 2018; 9: 827.

[16] Hosomi S, Grootjans J, Tschurtschenthaler M, Krupka N, Matute JD, Flak MB, Martinez-Naves E, Gomez Del Moral M, Glickman JN, Ohira M, Lanier LL, Kaser A and Blumberg R. Intestinal epithelial cell endoplasmic reticulum stress promotes MULT1 up-regulation and NKG2D-mediated inflammation. J Exp Med 2017; 214: 2985-2997.

[17] Raulet DH, Marcus A and Coscoy L. Dysregulated cellular functions and cell stress pathways provide critical cues for activating and targeting natural killer cells to transformed and infected cells. Immunol Rev 2017; 280: 93-101.

[18] Groh V, Bahram S, Bauer S, Herman A, Beauchamp M and Spies T. Cell stress-regulated human major histocompatibility complex class I gene expressed in gastrointestinal epithelium. Proc Natl Acad Sci U S A 1996; 93: 12445-12450.

[19] Gasser S, Orsulic S, Brown EJ and Raulet DH. The DNA damage pathway regulates innate immune system ligands of the NKG2D receptor. Nature 2005; 436: 1186-1190.

[20] Cerboni C, Zingoni A, Cippitelli M, Piccoli M, Frati L and Santoni A. Antigen-activated human T lymphocytes express cell-surface NKG2D ligands via an ATM/ATR-dependent mechanism and become susceptible to autologous NK- cell lysis. Blood 2007; 110: 606-615.

[21] Venkataraman GM, Suciu D, Groh V, Boss JM and Spies T. Promoter region architecture and transcriptional regulation of the genes for the MHC class I-related chain A and B ligands of NKG2D. J Immunol 2007; 178: 961-969.

[22] Zuo J, Mohammed F and Moss P. The biological influence and clinical relevance of polymorphism within the NKG2D ligands. Front Immunol 2018; 9: 1820.

[23] Nausch N and Cerwenka A. NKG2D ligands in tumor immunity. Oncogene 2008; 27: 5944-5958.

[24] Bui JD, Carayannopoulos LN, Lanier LL, Yokoyama WM and Schreiber RD. IFN-dependent down-regulation of the NKG2D ligand H60 on tumors. J Immunol 2006; 176: 905-913.

[25] Schwinn N, Vokhminova D, Sucker A, Textor S, Striegel S, Moll I, Nausch N, Tuettenberg J, Steinle A, Cerwenka A, Schadendorf D and Paschen A. Interferon-gamma down-regulates NKG2D ligand expression and impairs the NKG2D-mediated cytolysis of MHC class I-deficient melanoma by natural killer cells. Int J Cancer 2009; 124: 1594-1604.

[26] Yadav D, Ngolab J, Lim RS, Krishnamurthy S and Bui JD. Cutting edge: down-regulation of MHC class I-related chain A on tumor cells by IFN-gamma-induced microRNA. J Immunol 2009; 182: 39-43.

[27] Zhang C, Niu J, Zhang J, Wang Y, Zhou Z, Zhang J and Tian Z. Opposing effects of interferon-alpha and interferon-gamma on the expression of major histocompatibility complex class I chain-related A in tumors. Cancer Sci 2008; 99: 1279-1286.

[28] Diefenbach A and Raulet DH. Strategies for target cell recognition by natural killer cells. Immunol Rev 2001; 181: 170-184.
[29] Houchins JP, Yabe T, McSherry C and Bach FH. DNA sequence analysis of NKG2, a family of related cDNA clones encoding type II integral membrane proteins on human natural killer cells. J Exp Med 1991; 173: 1017-1020.
[30] Zuo J, Willcox CR, Mohammed F, Davey M, Hunter S, Khan K, Antoun A, Katakia P, Croudace J, Inman C, Parry H, Briggs D, Malladi R, Willcox BE and Moss P. A disease-linked ULBP6 polymorphism inhibits NKG2D-mediated target cell killing by enhancing the stability of NKG2D ligand binding. Sci Signal 2017; 10: eaai8904.
[31] Bedel R, Thiery-Vuillemin A, Grandclement C, Balland J, Remy-Martin JP, Kantelip B, Pallandre JR, Pivot X, Ferrand C, Tiberghien P and Borg C. Novel role for STAT3 in transcriptional regulation of NK immune cell targeting receptor MICA on cancer cells. Cancer Res 2011; 71: 1615-1626.
[32] Kryczek I, Wei S, Gong W, Shu X, Szeliga W, Vatan L, Chen L, Wang G and Zou W. Cutting edge: IFN-gamma enables APC to promote memory Th17 and abate Th1 cell development. J Immunol 2008; 181: 5842-5846.
[33] Lee SJ, Jang BC, Lee SW, Yang YI, Suh SI, Park YM, Oh S, Shin JG, Yao S, Chen L and Choi IH. Interferon regulatory factor-1 is prerequisite to the constitutive expression and IFN-gamma-induced upregulation of B7-H1 (CD274). FEBS Lett 2006; 580: 755-762.
[34] Garcia-Diaz A, Shin DS, Moreno BH, Saco J, Escuin-Ordinas H, Rodriguez GA, Zaretsky JM, Sun L, Hugo W, Wang X, Parisi G, Saus CP, Torrejon DY, Graeber TG, Comin-Anduix B, Hu-Lieskovan S, Damoiseaux R, Lo RS and Ribas A. Interferon receptor signaling pathways regulating PD-L1 and PD-L2 expression. Cell Rep 2017; 19: 1189-1201.
[35] Jinushi M, Takehara T, Kanto T, Tatsumi T, Groh V, Spies T, Miyagi T, Suzuki T, Sasaki Y and Hayashi N. Critical role of MHC class I-related chain A and B expression on IFN-alpha-stimulated dendritic cells in NK cell activation: impairment in chronic hepatitis C virus infection. J Immunol 2003; 170: 1249-1256.
[36] Molinero LL, Fuertes MB, Girart MV, Fainboim L, Rabinovich GA, Costas MA and Zwirner NW. NF-kappa B regulates expression of the MHC class I-related chain A gene in activated T lymphocytes. J Immunol 2004; 173: 5583-5590.
[37] Maasho K, Opoku-Anane J, Marusina AI, Coligan JE and Borrego F. NKG2D is a costimulatory receptor for human naive CD8+ T cells. J Immunol 2005; 174: 4480-4484.
[38] Pardoll DM. Immunology. Stress, NK receptors, and immune surveillance. Science 2001; 294: 534-536.
[39] Cerboni C, Ardolino M, Santoni A and Zingoni A. Detuning CD8+ T lymphocytes by down-regulation of the activating receptor NKG2D: role of NKG2D ligands released by activated T cells. Blood 2009; 113: 2955-2964.
[40] Verneris MR, Karimi M, Baker J, Jayaswal A and Negrin RS. Role of NKG2D signaling in the cytotoxicity of activated and expanded CD8+ T cells. Blood 2004; 103: 3065-3072.
[41] Zhang C, Zhang J, Sun R, Feng J, Wei H and Tian Z. Opposing effect of IFNgamma and IFNalpha on expression of NKG2 receptors: negative regulation of IFNgamma on NK cells. Int Immunopharmacol 2005; 5: 1057-1067.
[42] Shen J, Pan J, Du C, Si W, Yao M, Xu L, Zheng H, Xu M, Chen D, Wang S, Fu P and Fan W. Silencing NKG2D ligand-targeting miRNAs enhances natural killer cell-mediated cytotoxicity in breast cancer. Cell Death Dis 2017; 8: e2740.
[43] Xie J, Liu M, Li Y, Nie Y, Mi Q and Zhao S. Ovarian tumor-associated microRNA-20a decreases natural killer cell cytotoxicity by down-regulating MICA/B expression. Cell Mol Immunol 2014; 11: 495-502.
[44] Tsukerman P, Stern-Ginossar N, Gur C, Glasner A, Nachmani D, Bauman Y, Yamin R, Vitenshtein A, Stanietsky N, Bar-Mag T, Lankry D and Mandelboim O. MiR-10b downregulates the stress-induced cell surface molecule MICB, a critical ligand for cancer cell recognition by natural killer cells. Cancer Res 2012; 72: 5463-5472.
[45] Rohner A, Langenkamp U, Siegler U, Kalberer CP and Wodnar-Filipowicz A. Differentiation-promoting drugs up-regulate NKG2D ligand expression and enhance the susceptibility of acute myeloid leukemia cells to natural killer cell-mediated lysis. Leuk Res 2007; 31: 1393-1402.
[46] Xu Y, Zhou L, Zong J, Ye Y, Chen G, Chen Y, Liao X, Guo Q, Qiu S, Lin S, Chen H and Pan J. Decreased expression of the NKG2D ligand ULBP4 may be an indicator of poor prognosis in patients with nasopharyngeal carcinoma. Oncotarget 2017; 8: 42007-42019.
[47] Groh V, Smythe K, Dai Z and Spies T. Fas-ligand-mediated paracrine T cell regulation by the receptor NKG2D in tumor immunity. Nat Immunol 2006; 7: 755-762.

Supplementary Material

Supplementary data

RNA sequencing data of 113 patients with NPC from GEO database (Attachment Supplementary Table 1)

General information and clinical outcomes of patients enrolled

There were totally 57 patients with NPC enrolled, which include 40 males and 17 females. The median age at diagnosis was 46-year-old (ranges from 12 to 79 years). According to the 8th edition of the Union International Against Cancer (UICC)/American Joint Committee on Cancer (AJCC) system (1), 42 out of 57 (74%) patients were at stage III and 15 out of 57 (26%) patients were at stage IVA. Pathology proved undifferentiated non-keratinizing carcinoma was diagnosed in all 57 patients.

The average follow-up time was 121 months (ranges from 15 to 129 months). 4 out of 57 (7%) patients had local recurrence in the nasopharynx, 4/57 (7%) patients had local recurrence in regional lymph node and 12 out of 57 (21.1%) patients had distant metastasis. The median overall survival time and the median disease-free survival time after the initial treatment was both 121 months. The 5-year Overall Survival (OS) Rates and the 5-year Disease-Free Survival (DFS) rates were 73.7% and 68.4% respectively.

The concise baseline characteristics of patients enrolled were shown in Supplementary Table 2. The entire baseline characteristics and clinical outcomes were shown in attachment Supplementary Table 3.

Scores of immunohistochemistry staining of patients enrolled (Attachment Supplementary Table 4)

Prognostic and predictive values of ULBP3 in NPC

The univariate survival analyses (Supplementary Table 5) showed that clinical stage, T stage, expression of CD8 and ULBP3 protein were the influencing factors of OS in patients with NPC, and the expression of ULBP3 was also the influencing factor of DFS in patients with NPC. Sex, age, N stage and the expression of PD-L1 protein were not associated with prognosis.

The survival curves (Supplementary Figure 4) showed that OS in patients with high expression of CD8 protein was significantly longer than that in patients with negative/low expression of CD8. DFS and OS in patients with high expression of ULBP3 were both significantly longer than those in patients with negative/low expression of ULBP3.

In addition, we stained and analyzed the baseline tumor samples of some patients with advanced NPC who received the PD-1 inhibitors in our center. In the immune microenvironment of one patient primarily resistant to PD-1 inhibitor, we found a large number of infiltrated CD8$^+$ T cells, a strong expression of PD-L1 and an loss of expression of ULBP3 (Supplementary Figure 5A). In addition, in another sample of one patient who responded to PD-1 inhibitor, we found a similar infiltration of CD8$^+$ T cell, a positive expression of PD-L1 whereas a positive expression of ULBP3 (Supplementary Figure 5B).

Reference

[1] N. C. C. Network: National Comprehensive Cancer Network. (NCCN) Clinical Practice Guidelines in Oncology. Head and Neck Cancer, Version 2. In, (2018).

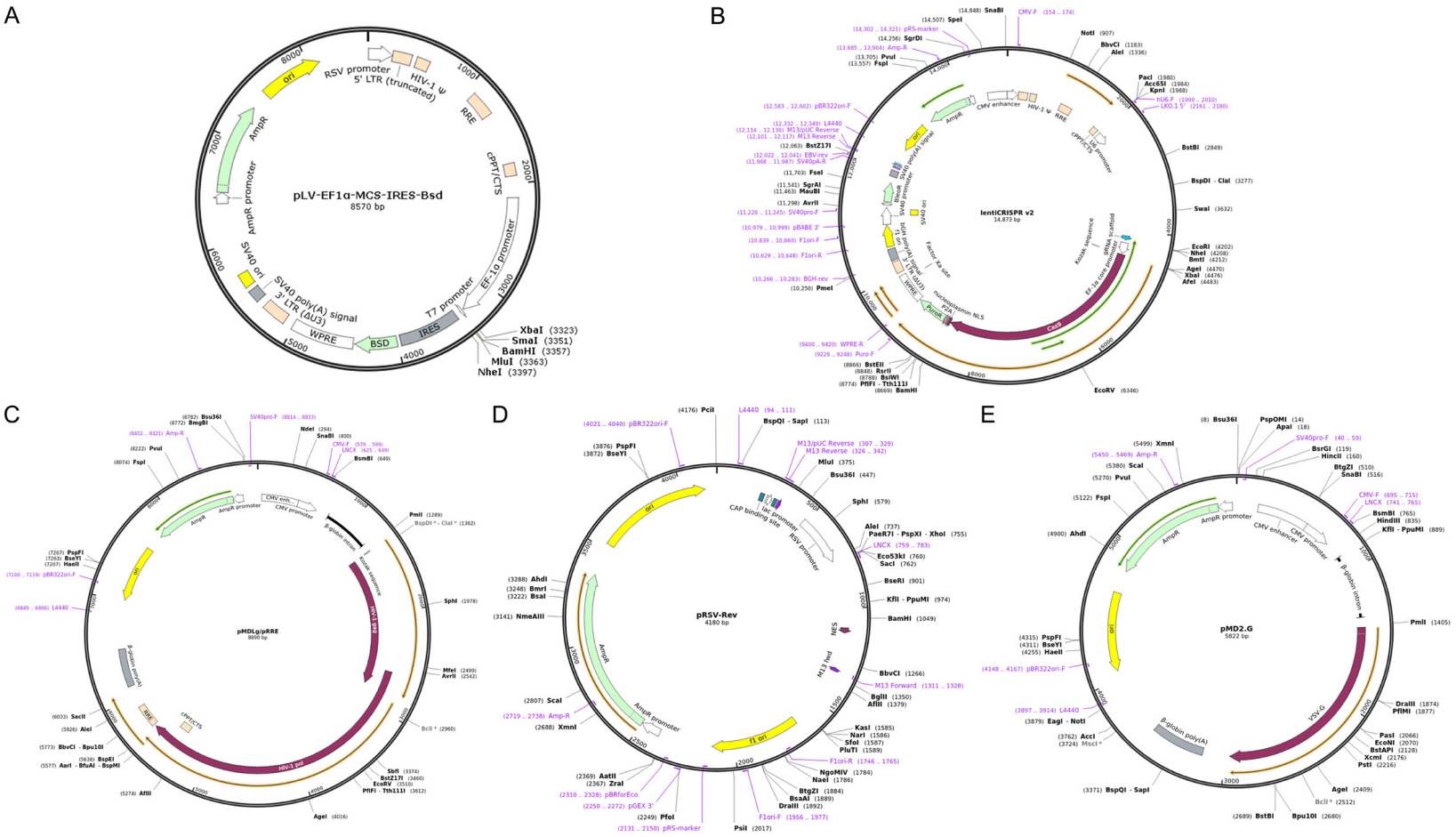

Supplementary Figure 1. Structures of plasmids used in our study. A. pLV-EF1a-MCS-Flag-IRES-Bsd; B. Lenticrispr V2; C. pMDLg/pRRE; D. pRSV-Rev; E. pMD2.G.

Supplmentary Table 2. Baseline characteristics of patients enrolled (N=57)

Baseline characteristics		n (%)
Gender	Female	17 (30%)
	Male	40 (70%)
Age	≥50	22 (39%)
	<50	35 (61%)
Median age	46 (12~79)	
Clinical stage	I	0
	II	0
	III	42 (74%)
	IVA	15 (26%)
	IVB	0
T stage	1	0
	2	6 (11%)
	3	41 (72%)
	4	10 (17%)
N stage	0	10 (17%)
	1	24 (42%)
	2	17 (30%)
	3	6 (11%)

Supplmentary Table 4. The scores of immunohistochemistry staining of 57 cases of samples

No.	CD8			PD-L1			ULBP3		
	First Score (%)	Second Score (%)	Final Score (%)	First Score (CPS)	Second Score (CPS)	Final Score (CPS)	First Score (CPS)	Second Score (CPS)	Final Score (CPS)
1	60	70	65	90	20	20	4	1	1
2	80	70	75	90	70	70	<1	<1	0
3	55	45	45	0	0	0	<1	<1	0
4	75	75	75	60	30	30	<1	<1	0
5	70	50	45	<5	<1	0	5	5	7
6	75	60	45	5	<1	0	7	6	6
7	85	60	30	5	<1	0	0	0	0
8	50	25	15	20	8	8	<1	0	0
9	5	<1	1	0	0	0	1	1	1
10	25	10	10	0	0	0	<1	<1	0
11	45	30	15	5	2	2	1	1	1
12	10	<1	1	0	0	0	5	5	6
13	80	65	65	0	0	0	45	45	45
14	25	10	10	15	10	10	5	5	6
15	45	10	10	10	0	0	0	0	0
16	85	75	75	15	20	20	0	0	0
17	40	25	25	<1	0	0	7	7	7
18	5	2	2	0	0	0	<1	0	0
19	80	80	80	50	20	20	<1	<1	0
20	10	8	8	20	5	5	0	0	0
21	80	55	40	70	15	20	1	1	1
22	90	65	40	70	10	20	<1	<1	0
23	15	8	8	0	0	0	5	5	6
24	75	50	50	40	0	0	0	0	0
25	45	35	35	30	20	15	10	10	10
26	10	1	1	20	15	15	5	5	6
27	50	30	30	60	35	35	1	1	1
28	70	50	50	<5	1	1	<1	0	0
29	70	60	40	>20	10	10	<1	0	0
30	70	50	50	<5	<1	0	<1	<1	0
31	10	3	1	20	1	1	15	15	15
32	65	50	50	0	<1	0	1	1	1
33	65	50	40	20	5	5	<1	0	0
34	75	70	70	0	0	0	15	15	15
35	55	30	30	30	20	20	<1	<1	0
36	70	45	45	<10	1	1	25	25	25
37	90	65	65	<30	5	5	5	5	6
38	30	30	30	30	15	15	5	5	6
39	75	20	20	5?	0	0	<1	<1	0
40	80	60	60	<30	10	20	1	0	1
41	75	50	50	>90	30	30	1	1	1
42	80	70	70	20	10	20	5	5	5
43	65	60	60	80	5	5	5	5	6
44	75	60	60	70	45	45	2	2	2
45	40	20	20	10	<1	1	<1	0	0
46	75	60	60	<40	10	20	1	1	1
47	60	50	50	<5	5	5	1	1	1
48	25	20	20	0	0	0	5	5	5

49	65	55	55	70	35	15	5	5	6
50	85	80	80	70	20	20	1	1	1
51	75	55	40	0	0	0	5	5	5
52	70	55	35	<10	1	1	1	1	1
53	50	35	35	<10	8	8	2	2	2
54	65	45	45	80	60	60	1	1	1
55	55	40	45	15	15	15	4	4	6
56	75	55	55	30	10	20	<1	0	0
57	60	45	45	90	50	50	0	0	0

Supplmentary Table 5. Univariate Survival Analysis of 57 patients enrolled

Variable		n	mDFS (m)	*p*-value	mOS (m)	*p*-value
Gender	Female	17	--	0.498	--	0.774
	Male	40	--		--	
Age	≥50	22	--	0.725	--	0.142
	<50	35	--		--	
Clinical stage	III	42	--	0.273	--	0.003
	IVA	15	--		61	
T stage	2	6	--	0.336	86	0.023
	3	41	--		--	
	4	10	--		30	
N stage	0	10	--	0.589	--	0.300
	1	24	--		--	
	2	17	--		--	
	3	6	--		61	
PD-L1	Negative/low-expression	39	--	0.649	--	0.571
	High-expression	18	--		--	
CD8	Negative/low-expression	28	--	0.229	--	0.042
	High-expression	29	--		--	
UBLP3	Negative/low-expression	40	--	0.036	--	0.033
	High-expression	17	--		--	

-- The median cumulative survival rate was not reached.

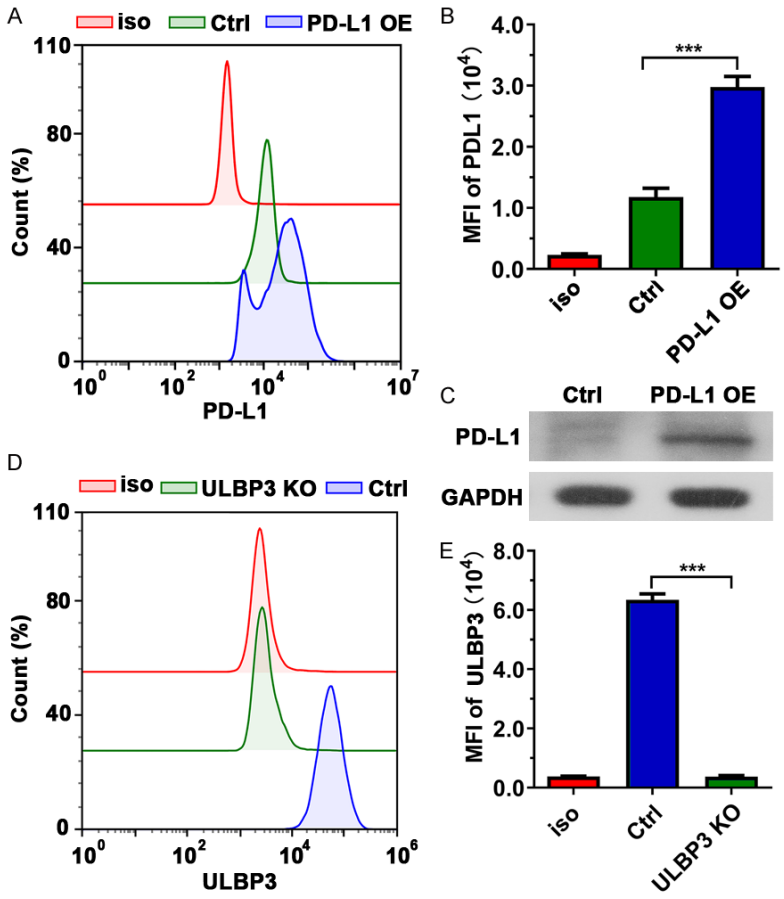

Supplementary Figure 2. Verification of 5-8F cell lines with different phenotypes. Results of FACS (A and B) and western blotting (C) indicated that the expression of PD-L1 was significantly higher than the control cells; (D and E) Detection of ULBP3 in 5-8F cell line which transfected with ULBP3 knockout plasmid and control and isotype cell line. Results of FACS indicated that the expression of ULBP3 was significantly lower than the control cells. ***P<0.001.

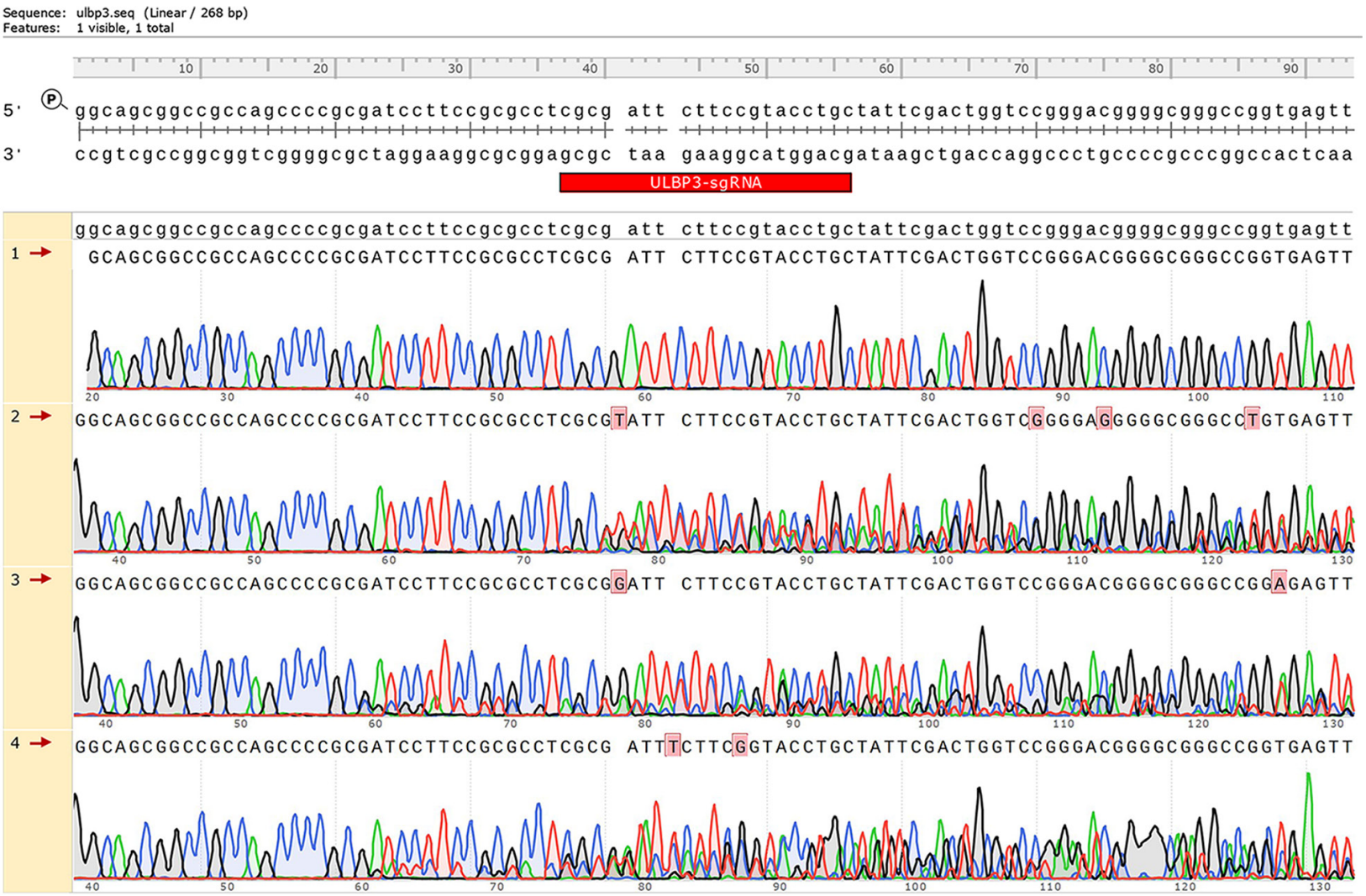

Supplementary Figure 3. Verification of the genetic knockout in 5-8F cell lines.

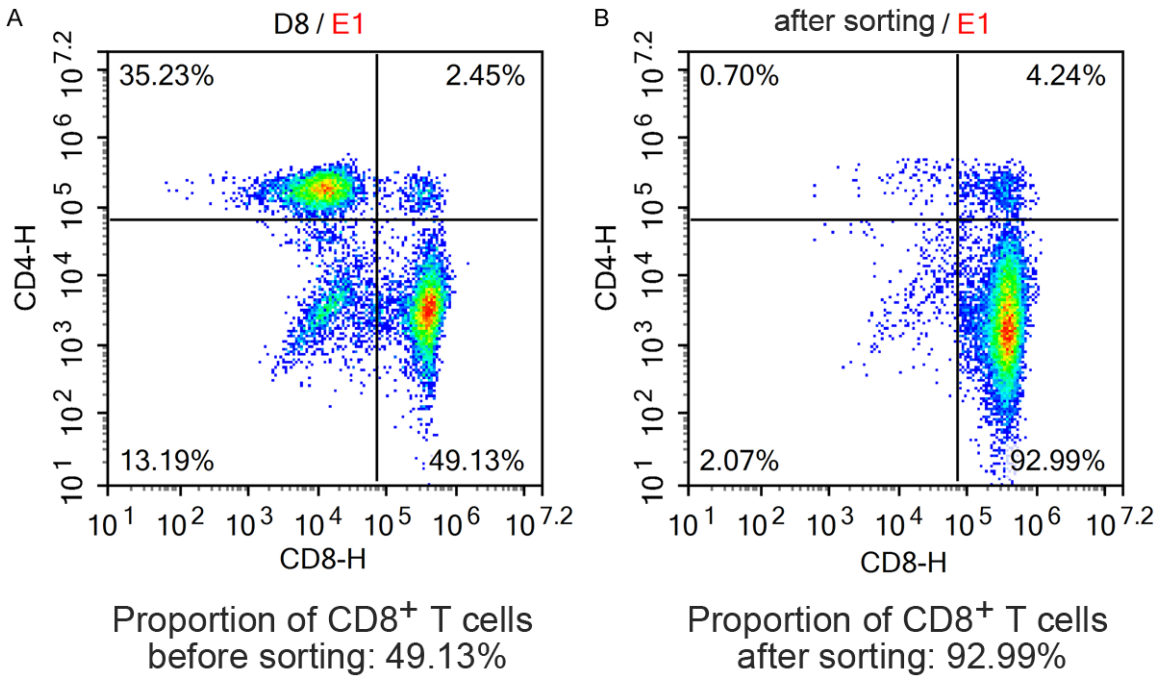

Supplementary Figure 4. Detection of proportion of 5-8F-specific $CD8^+$ T cells. A. The proportion of 5-8F-specific $CD8^+$ T cells before sorting was 49.13%. B. The proportion of 5-8F-specific $CD8^+$ T cells after sorting was 92.17%, which was significantly higher than that before sorting.

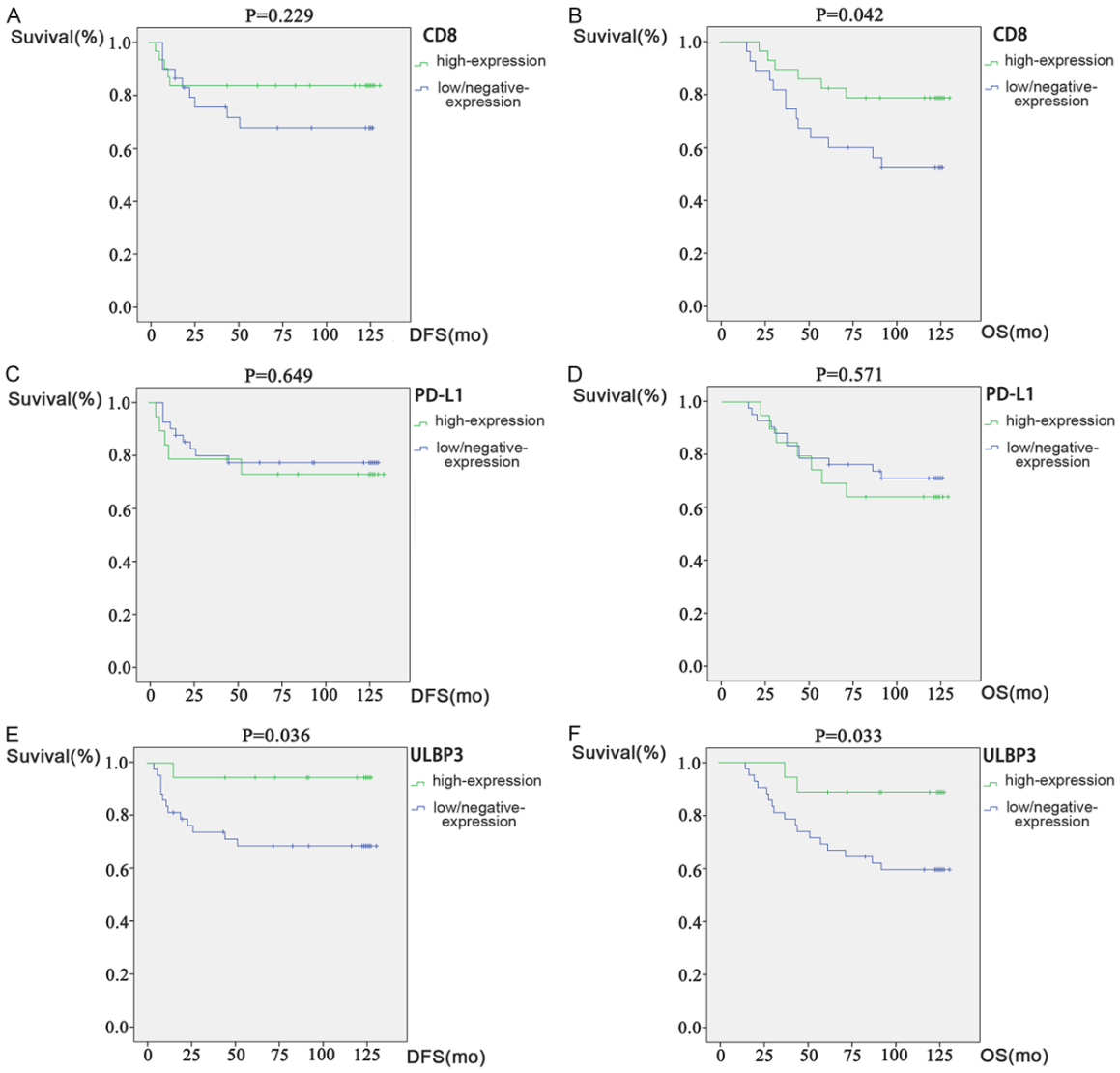

Supplementary Figure 5. Effects of PD-L1, CD8 and ULBP3 on survival in 57 patients with NPC. Green line: high-expression; blue line: negative/low-expression. A. The expression of CD8 protein had no significant effect on DFS in NPC. B. The OS of patients with high-expression of CD8 was significantly longer than that of patients with negative/low-expression (P<0.042). C. The expression of PD-L1 protein in NPC had no significant effect on DFS. D. The expression of PD-L1 protein in NPC had no significant effect on OS. E. The DFS of patients with high-expression of ULBP3 was significantly longer than that of patients with negative/low-expression (P<0.036). F. The OS of patients with high-expression of ULBP3 was significantly longer than that of patients with negative/low-expression (P<0.033).

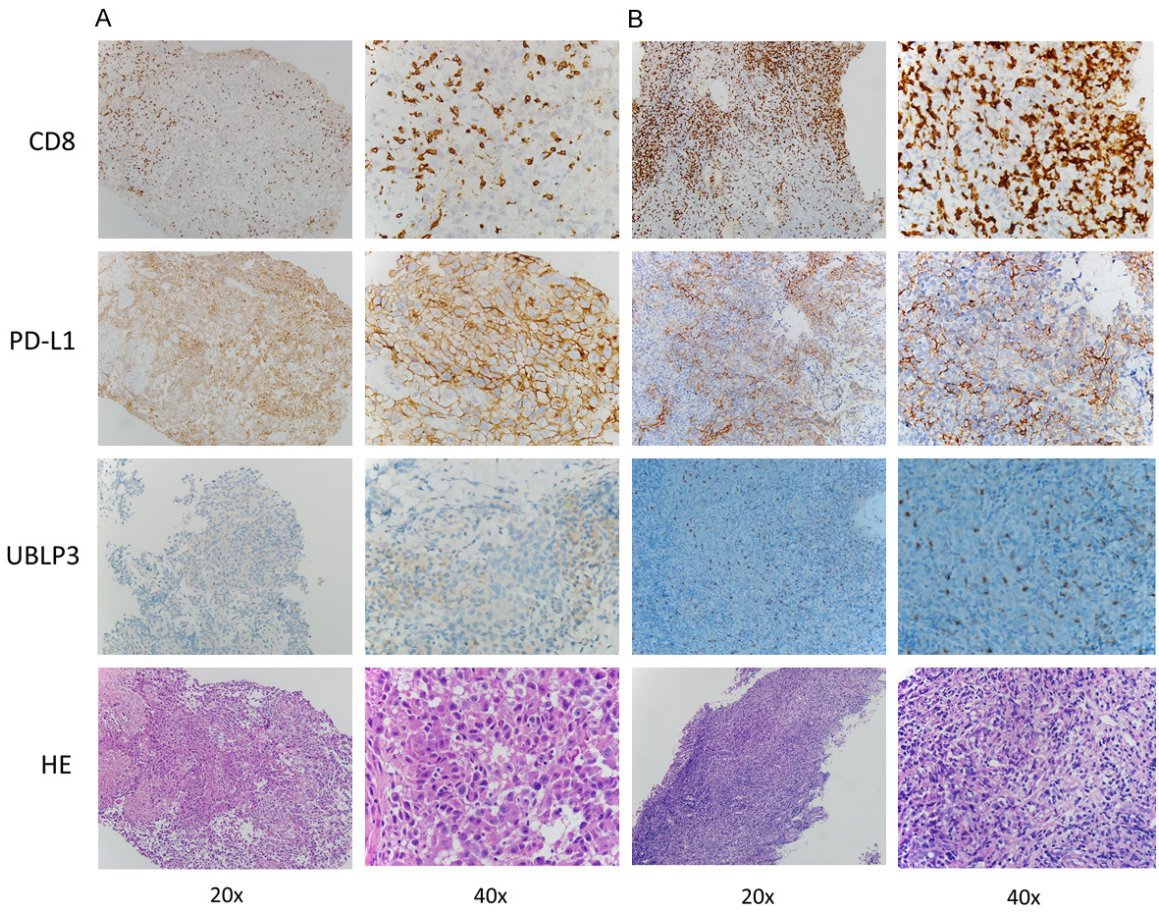

Supplementary Figure 6. IHC staining of 2 patients with NPC received PD-1 inhibitors. A. In microenvironment of this patient with primary resistance to PD-1 inhibitor, the expression of CD8 and PD-L1 was high and the expression of ULBP3 was negative; B. In microenvironment of this patient with effective response to PD-1 inhibitor, the expression of PD-L1 was high and the expression of ULBP3 was positive.